

## Magnetic correlations in oxides: Neutron diffraction and neutron depolarization study

S M YUSUF

Solid State Physics Division, Bhabha Atomic Research Centre, Mumbai 400 085, India  
E-mail: smyusuf@barc.gov.in

**Abstract.** We have studied magnetic correlations in several oxide materials that belong to colossal magnetoresistive, naturally occurring layered oxide showing low-dimensional magnetic ordering, solid oxide fuel cell interconnect materials, and magnetic nanoparticles using neutron diffraction and neutron depolarization techniques. In this paper, an overview of some of these results is given.

**Keywords.** Magnetic oxides; neutron diffraction; neutron depolarization; magnetic correlations.

**PACS Nos** 75.25.+z; 75.50.-y

### 1. Introduction

The importance of magnetic oxides has shown a spectacular increase in the last few decades. The oxide materials are known to exhibit various interesting physical properties such as high-temperature superconductivity, multiferroic behaviour, colossal magnetoresistance (CMR) effect, room temperature ferro/ferrimagnetic ordering in nanoparticles, naturally occurring layered materials showing exotic physical properties, interconnect and cathode materials in solid oxide fuel cells. We have studied magnetic correlations in a large number of oxide materials [1–8] as a function of temperature and magnetic field using neutron diffraction and neutron depolarization techniques. These oxide materials are of wide varieties, such as, CMR materials, low-dimensional magnetic materials, solid oxide fuel cell (SOFC) materials, magnetic nanoparticles, etc. In this article we describe the results of some of these investigations that have been made using the neutron instruments at Dhruva reactor, Trombay [9,10] and other neutron scattering facilities, located in Europe.

### 2. Experimental

All the samples (except  $\gamma$ -Fe<sub>2</sub>O<sub>3</sub>) studied in this paper were polycrystalline in nature and were prepared by the solid state reaction method. The neutron diffraction measurements were carried out at Dhruva reactor, Trombay [9] and other

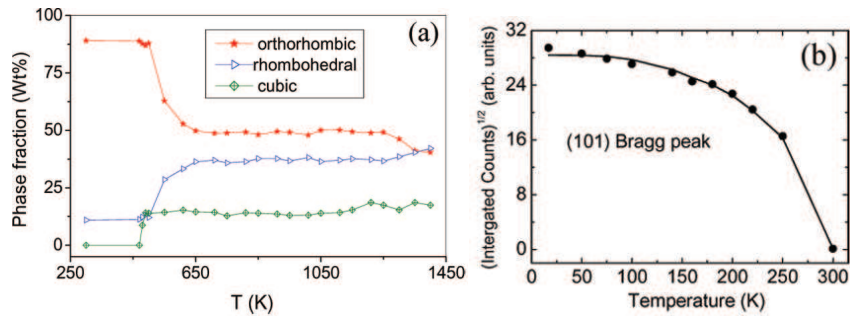


**Figure 1.** (a) Weight % of various phases for  $\text{La}_{0.75}\text{Sr}_{0.25}\text{CrO}_3$ . (b) Square root of the integrated Bragg intensity of (101) vs.  $T$ , fitted to the mean field theory.

neutron scattering facilities, located elsewhere. The neutron depolarization experiments were performed using the polarized neutron spectrometer [10] at the Dhruva reactor.

### 3. Results and discussion

#### 3.1 $\text{La}_{0.75}\text{Sr}_{0.25}\text{CrO}_3$ : A high- and low-temperature neutron diffraction study

Sr-doped  $\text{LaCrO}_3$  compounds have been mainly studied for their use as interconnects in SOFCs [1]. If the structural phase transition temperature lies close to the SOFC operation temperature it can affect the mechanical integrity of the SOFC device. Structural study is, therefore, important to understand the details of the structural phase transitions.

In this article, we present the results of our structural study for 25 mol%  $\text{Sr}^{2+}$ -doped  $\text{LaCrO}_3$  compound, carried out using the HRPT diffractometer (high-resolution powder diffractometer using thermal neutrons) over  $300 \text{ K} \leq T \leq 1400 \text{ K}$  at the Paul Scherrer Institut. We performed Rietveld refinement of the diffraction patterns. Figure 1a shows the evolution of weight percentages of the three phases as a function of temperature. We find that the phase fractions show almost no change over 1073 K to 1173 K, the operating temperature region for its use as an interconnect material in the SOFC technology.

Figure 2 depicts the low-angle Bragg peak intensities as a function of temperature. The magnetic peaks were visible up to 250 K and disappeared at  $\sim$  room temperature (RT), indicating the Néel temperature to be between 250 K and RT. The Rietveld refinement shows that the  $\text{Cr}^{3+}$  ionic moments are aligned in a G-type antiferromagnetic structure and ordered along the  $b$ -axis. The  $\text{Cr}^{3+}$  ions, located at  $(1/2, 0, 0)$  and  $(0, 1/2, 1/2)$  have parallel spins and are aligned oppositely to the  $\text{Cr}^{3+}$  ionic moments, located at  $(0, 1/2, 0)$  and  $(1/2, 0, 1/2)$ . The chemical and magnetic unit cells are of the same dimension. At 17 K, the site averaged Cr-moment is found to be  $2.71(5) \mu_B$  per Cr ion. The theoretically expected spin-only ordered moments for  $\text{Cr}^{3+}$  and  $\text{Cr}^{4+}$  are 3 and  $2 \mu_B$ , respectively. The observed value of

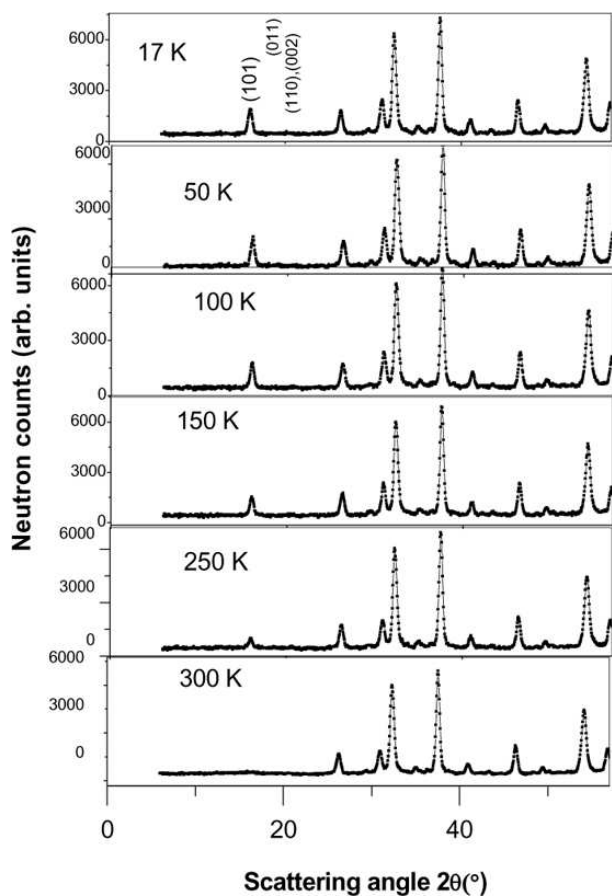


**Figure 2.** Neutron diffraction patterns with  $\lambda = 1.249 \text{ \AA}$ .

moment ( $2.71(5) \mu_B$  per Cr ion) is very close to the weighted average of the spin-only moment of  $2.75 \mu_B$  originated from 75 atomic%  $\text{Cr}^{3+}$  ( $2.25 \mu_B$ ) and 25 atomic%  $\text{Cr}^{4+}$  ( $0.50 \mu_B$ ). Figure 1b shows a plot of the square root of the integrated intensity of the (101) reflection as a function of temperature. The temperature variation of the intensity has shown a Brillouin function dependence with  $J = 1.375$  in the mean field theory.

### 3.2 Field induced ferromagnetism in $(\text{La}/\text{Dy})_{0.7}\text{Ca}_{0.3}\text{MnO}_3$ CMR perovskite

We have performed a magnetic study on the  $(\text{La}_{1-x}\text{Dy}_x)_{0.7}\text{Ca}_{0.3}\text{MnO}_3$  system. Substitution of  $\text{La}^{3+}$  by  $\text{Dy}^{3+}$  in  $\text{La}_{0.7}\text{Ca}_{0.3}\text{MnO}_3$  keeps the ratio of  $\text{Mn}^{3+}/\text{Mn}^{4+}$  unaltered to its original value. Our neutron diffraction study at the Dhruva reactor shows that if  $\text{La}^{3+}$  (ionic radius =  $1.06 \text{ \AA}$ ) is replaced by a smaller Dy ion (ionic radius =  $0.91 \text{ \AA}$ ), the buckling of the  $\text{MnO}_6$  octahedra (orthorhombic

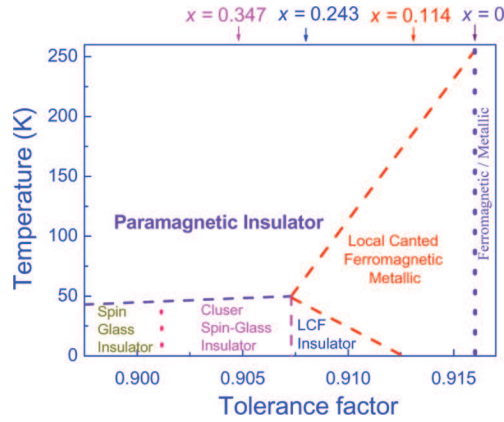


**Figure 3.** Magnetic and electronic phase diagram for  $(\text{La}_{1-x}\text{Dy}_x)_{0.7}\text{Ca}_{0.3}\text{MnO}_3$ .

distortion) increases. The buckling gives a weaker ferromagnetic double-exchange interaction. These ferromagnetic interactions compete with the coexisting  $t_{2g}(\text{Mn})-2p_{\pi}(\text{O})-t_{2g}(\text{Mn})$  superexchange antiferromagnetic interactions and drive the systems towards a local canted ferromagnetic (LCF) state. A higher substitution of Dy leads to a cluster spin glass (CSG) and then to a spin-glass state. Based on these results [2], obtained using the facilities at our centre, we propose here a magnetic and electronic phase diagram as a function of the tolerance factor  $t$  for the perovskite structure, defined as  $t = (r_A + r_O)/\sqrt{2}(r_B + r_O)$ , where  $r_A$  is the average ionic radius of (La/Ca/Dy) site,  $r_O$  is the ionic radius of  $\text{O}^{2-}$ , and  $r_B$  is the average ionic radius of ions at the B (Mn) site (figure 3).

Now we present the results of magnetic field-dependent neutron diffraction study (carried out at ILL, Grenoble using the D16 instrument with  $\lambda = 4.54 \text{ \AA}$ ) on the higher Dy-substituted,  $x = 0.347$  sample which shows a CSG behaviour (figure 3). The diffraction patterns have been plotted as a function of field and temperature in figure 4 where a field-induced transition from a CSG to a ferromagnetic state is evident [2].

### 3.3 Neutron depolarization study of $(\text{Nd}_{1-x}\text{Tb}_x)_{0.55}\text{Sr}_{0.45}\text{MnO}_3$ perovskites

The temperature dependence of the transmitted neutron beam polarization  $P_f$  [7,8,10] in 1D ( $z-z$ ) neutron depolarization study for the  $(\text{Nd}_{1-x}\text{Tb}_x)_{0.55}\text{Sr}_{0.45}\text{MnO}_3$  perovskites under an applied field of 10 Oe is depicted in figure 5. For the  $x = 0.3, 0.5, 0.53$  and  $0.56$  samples  $P_f$  shows a sharp decrease below  $\sim 170, 98, 70$  and  $65$  K, respectively. For the  $x = 0.6$  sample, a very small decrease of  $P_f$  is observed below  $\sim 113$  K. However, for the  $x = 0.7$  sample no depolarization is found. From the observed depolarization, an estimate of the average size of domains/clusters (table 1) was made using the procedure that was mentioned earlier [3,7,8,10]. The mean  $B$  values were obtained from the Arrott plot of DC magnetization [3].

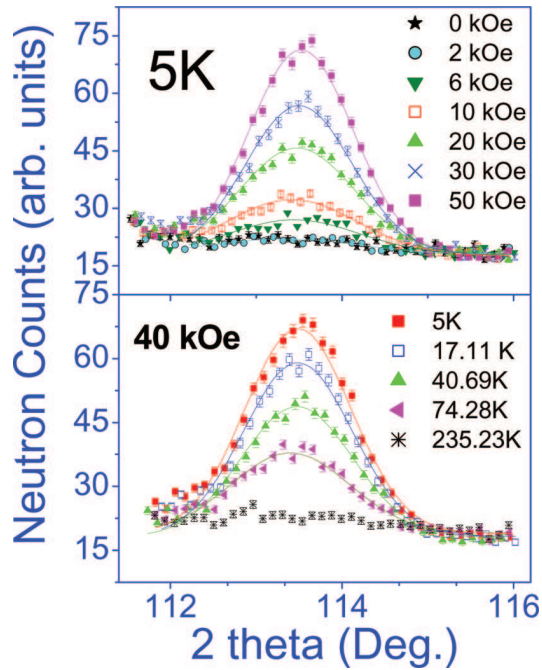


**Figure 4.** Evolution of the Bragg peaks as a function of temperature and magnetic field.

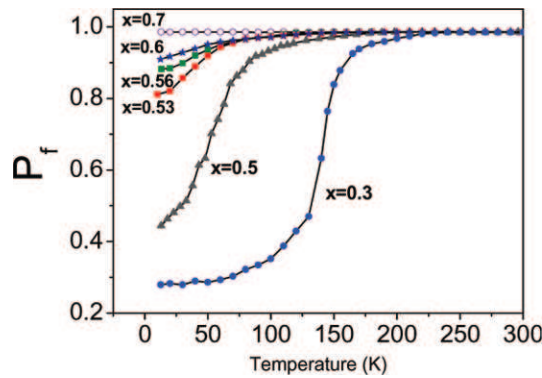


**Figure 5.**  $P_f$  vs.  $T$  for  $(\text{Nd}_{1-x}\text{Tb}_x)_{0.55}\text{Sr}_{0.45}\text{MnO}_3$ .

### 3.4 A 2D–3D cross-over of magnetic ordering in the bilayer manganite $\text{Ca}_{2.5}\text{Sr}_{0.5}\text{GaMn}_2\text{O}_8$

In low-dimensional systems, magnetic long-range ordering at finite temperature is possible if anisotropy is considered [4]. In this article we present the results of neutron diffraction study (carried out at LLB, Saclay with  $\lambda = 4.741 \text{ \AA}$ ) for  $\text{Ca}_{2.5}\text{Sr}_{0.5}\text{GaMn}_2\text{O}_8$ , an Mn-based bilayered oxide compound. The compound has

**Table 1.** The spontaneous magnetization  $M_{\text{Sp}}$ , magnitude of average internal magnetic induction  $B$ , and average magnetic domain size  $\Delta$  for  $(\text{Nd}_{1-x}\text{Tb}_x)_{0.55}\text{Sr}_{0.45}\text{MnO}_3$ .

$x$	$M_{\text{Sp}}$ ( $\mu_{\text{B}}/\text{f.u.}$ )	$B$ (G)	$\Delta$ ( $\mu\text{m}$ )
0.1	3.6054	7575.33	0.4293
0.3	4.0283	8402.36	0.5163
0.5	4.0997	8489.92	0.3339
0.53	4.1141	8510.42	0.0832
0.56	4.1286	8531.18	0.0473
0.6	4.1482	8559.58	0.0181

a perovskite structure where two  $\text{MnO}_6$  octahedra layers are separated by a single layer of  $\text{GaO}_4$  tetrahedra [4].

In figure 6, over 160–165 K, two saw-tooth type asymmetric magnetic Bragg peaks centred on  $2\theta \approx 51.3$  and  $52.7^\circ$  are observed. However, over 150–155 K, the saw-tooth type peaks gradually disappear and symmetric Bragg peaks appear. Over the range 150–155 K, the symmetric Bragg peaks at  $2\theta = 51.54(1)$ ,  $52.91(1)$ ,  $57.67(5)$ , and  $58.95(5)^\circ$  have been indexed as (100), (001), (110) and (011), respectively, signalling that a 3D long-range antiferromagnetic correlation has built up. The ordered Mn moments are aligned along the [010] direction. Following Warren [5], the diffracted intensity for the ( $hl$ ) 2D Bragg reflection has been calculated numerically to fit the experimental data over 160–165 K. The mean 2D correlation length  $\xi$  was found to be 325 and 550 Å at 165 and 160 K, respectively. At  $T < 150$  K ( $T_{\text{N-3D}}$ ) the 3D Bragg peak widths are limited by the instrumental  $Q$  resolution. The asymmetric saw-tooth type Bragg peaks, observed at  $2\theta = 51.30$  and  $52.70^\circ$ , are indexed as ( $h = 1, l = 0$ ) and ( $h = 0, l = 1$ ), respectively. The present work establishes the 2D–3D magnetic ordering cross-over phenomenon in a system where 3d transition metal (Mn) magnetism, and superexchange interactions are involved, giving a unique example of superexchange mediated magnetic ordering dimensionality cross-over in a layered material.

### 3.5 Structural and magnetic study of nanoparticles of $\gamma\text{-Fe}_2\text{O}_3$

Iron oxides attract a great deal of interest due to their technological importance in information storage, ferrofluids, biomedical applications, etc. The nanoparticles of  $\gamma\text{-Fe}_2\text{O}_3$  have been prepared using a reverse micelle technique [6]. The transmission electron microscope (TEM) image (figure 7) confirms the formation of nanoparticles with an average radius of  $\sim 5.1$  nm.

Figure 8 depicts the observed and Rietveld refined neutron diffraction patterns at 297 and 17 K. It is interesting to note that nanoparticles of 5.1 nm radius are good enough to show such well-formed Bragg peaks. The Rietveld profile analysis demonstrated that the crystal structure could be refined using the  $\text{P4}_3\text{32}$  space group. There are two octahedral sites (12d and 4b) with 9.75 and 37.5% cation vacancies, respectively, with no vacancy at the 8c tetrahedral site. The cation

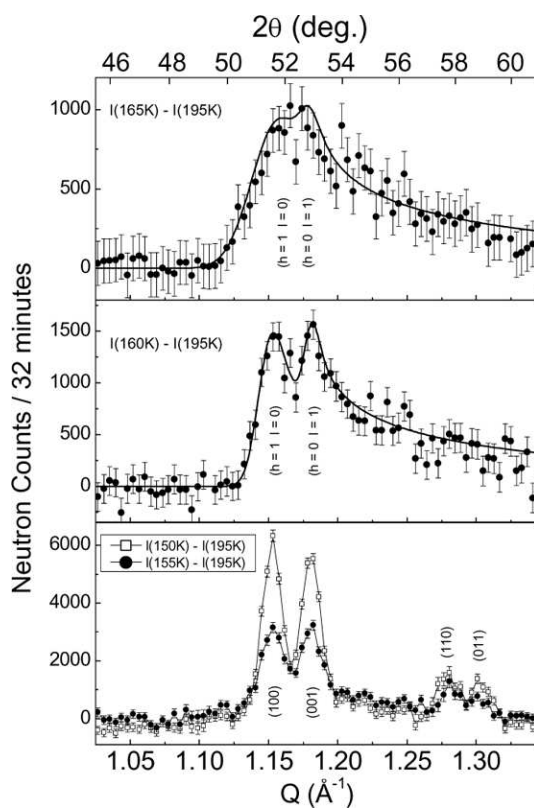


**Figure 6.** Diffraction patterns at 165, 160, 155 and 150 K (nuclear background corrected). Solid curves (in top two panels) are the calculated profiles using the 2D Warren function.

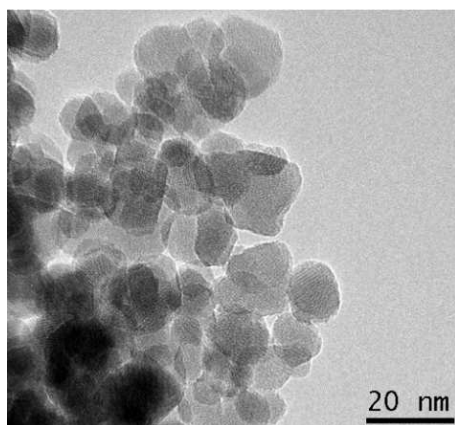


**Figure 7.** TEM image for the  $\gamma$ -Fe<sub>2</sub>O<sub>3</sub> sample.

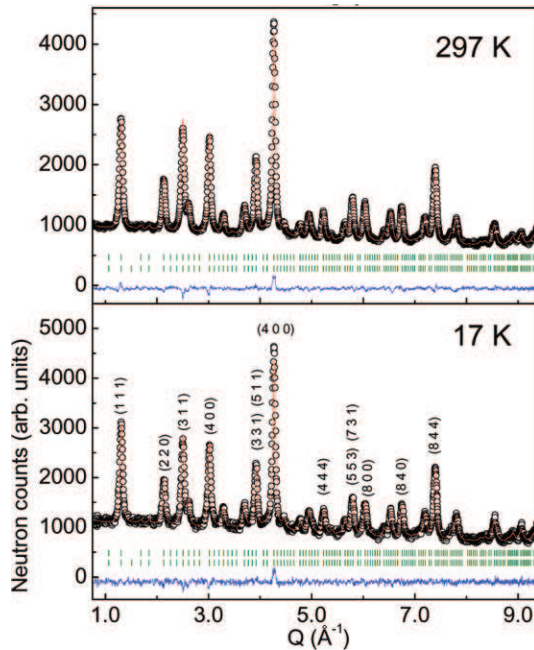


**Figure 8.** Rietveld refined neutron diffraction patterns at 297 and 17 K.

and oxygen occupancies maintain the 2:3 ratio corresponding to the  $\gamma$ - $\text{Fe}_2\text{O}_3$  compound. A ferrimagnetic ordering of tetrahedral and octahedral site moments has been observed at 297 and 17 K. There is a significant reduction of the tetrahedral and octahedral site moments (aligned along the unit cell axes) as compared to the theoretical value of  $5 \mu_{\text{B}}$  for  $\text{Fe}^{3+}$  ion. Surface spin disorder, arising from reduced coordination and broken exchange bonds, is expected to give a reduced magnetization.

#### 4. Summary and conclusion

We have investigated magnetic correlation in various oxides using neutron diffraction and neutron depolarization techniques. The samples studied here are important in the area of CMR effect, low-dimensional magnetism, nanomagnetism, and interconnect material for SOFC. Our study shows a field-induced transition of the cluster spin glass state to a ferromagnetic state for  $(\text{La}_{1-x}\text{Dy}_x)_{0.7}\text{Ca}_{0.3}\text{MnO}_3$  CMR perovskites with  $x = 0.347$ . A G-type antiferromagnetic structure involving the spin ordering of  $\text{Cr}^{3+}$  ionic moments for the SOFC interconnect compound  $\text{La}_{0.75}\text{Sr}_{0.25}\text{CrO}_3$  is found. The diffraction study on the  $\gamma$ - $\text{Fe}_2\text{O}_3$  nanoparticles shows a strong magnetic character (ferrimagnetism) at room temperature, a desired property for various applications including drug delivery. The naturally occurring layered oxide material  $\text{Ca}_{2.5}\text{Sr}_{0.5}\text{GaMn}_2\text{O}_8$  shows a novel dimensionality cross-over of magnetic ordering from 2D to 3D. The study also includes the determination of average magnetic domain size for  $(\text{Nd}_{1-x}\text{Tb}_x)_{0.55}\text{Sr}_{0.45}\text{MnO}_3$  CMR perovskites.

## Acknowledgment

This article is based on several collaborative works as evident from the cited references. The author acknowledges the valuable contributions of his collaborators.

## References

- [1] K R Chakraborty, S M Yusuf and P S R Krishna, *Pramana – J. Phys.* **63**, 251 (2004)  
K R Chakraborty, A Das, S M Yusuf, PSR Krishna and A K Tyagi, *J. Magn. Magn. Mater.* **301**, 74 (2006)  
K R Chakraborty, S M Yusuf, P S R Krishna, M Ramanadham, A K Tyagi and V Pomjakushin, *J. Phys.: Condens. Matter* **18**, 8661 (2006)  
K R Chakraborty, S M Yusuf, P S R Krishna, M Ramanadham, V Pomjakushin and A K Tyagi, *J. Phys.: Condens. Matter* **19**, 216207 (2007)  
K R Chakraborty, S M Yusuf and A K Tyagi, *J. Magn. Magn. Mater.* **320**, 1163 (2008)
- [2] S M Yusuf, K Chakraborty, S K Paranjpe, R Ganguly, P K Mishra, J V Yakhmi and V C Sahni, *Phys. Rev.* **B68**, 104421 (2003)  
S M Yusuf, R Ganguly, K Chakraborty, P K Mishra, S K Paranjpe, J V Yakhmi and V C Sahni, *J. Alloys Compounds* **326**, 89 (2001)  
S M Yusuf, K R Chakraborty, R Ganguly, P K Mishra, S K Paranjpe, J V Yakhmi and V C Sahni, *J. Magn. Magn. Mater.* **272–276**, 1288 (2004)  
S M Yusuf, J M De Teresa, C Ritter, D Serrate, M R Ibarra, J V Yakhmi and V C Sahni, *Phys. Rev.* **B74**, 144427 (2006)
- [3] S M Yusuf, J M De Teresa, P A Algarabel, J Blasco, M R Ibarra, A Kumar and C Ritter, *Physica* **B385–386**, 401 (2006)  
J M De Teresa, C Ritter, P A Algarabel, S M Yusuf, J Blasco, Amit Kumar, C Marquina and M R Ibarra, *Phys. Rev.* **B74**, 224442 (2006)
- [4] S M Yusuf, J M De Teresa, P A Algarabel, M D Mukadam, M J Mignot, I Mirebeau, C Marquina and R M Ibarra, *Phys. Rev.* **B74**, 184409 (2006)  
A Jain, Sher Singh and S M Yusuf, *Phys. Rev.* **B74**, 174419 (2006)  
I Nowik, A Jain, S M Yusuf and J V Yakhmi, *Phys. Rev.* **B77**, 054403 (2008)
- [5] B E Warren, *Phys. Rev.* **59**, 693 (1941)
- [6] S M Yusuf, J M De Teresa, M D Mukadam, J Kohlbrecher, M R Ibarra, J Arbiol, P Sharma and S K Kulshreshtha, *Phys. Rev.* **B74**, 224428 (2006)  
M D Mukadam, S M Yusuf, P Sharma and S K Kulshreshtha, *J. Magn. Magn. Mater.* **272–276**, 1401 (2004)
- [7] S M Yusuf, M Sahana, M S Hegde, K Dörr and K-H Müller, *Phys. Rev.* **B62**, 1118 (2000)  
A Das, M Sahana, S M Yusuf, L Madhav Rao, C Shivakumara and M S Hegde, *Mater. Res. Bull.* **35**, 651 (2000)  
S M Yusuf, M Sahana, K Dörr, U K Röbller and K H Müller, *Phys. Rev.* **B66**, 064414 (2002)  
S M Yusuf, *Pramana – J. Phys.* **63**, 133 (2004)  
S Röbller, U K Röbller, K Nenkov, D Eckert, S M Yusuf, K Dörr and K-H Müller, *Phys. Rev.* **B70**, 104417 (2004)  
D K Aswal, A Singh, C Thinaharan, S M Yusuf, C S Viswanatham, G L Goswami, L C Gupta, S K Gupta, J V Yakhmi and V C Sahni, *Philos. Magn.* **B83**, 3181 (2003)

- J S Srikiran and S M Yusuf, *J. Alloys Compounds* **390**, 26 (2005)  
J S Srikiran, A Kumar and S M Yusuf, *J. Magn. Magn. Mater.* **295**, 168 (2005)  
S P Singh, A K Singh, D Pandey and S M Yusuf, *Phys. Rev.* **B76**, 054102 (2007)  
[8] S M Yusuf, V C Sahni and L Madhav Rao, *J. Phys.: Condens. Matter* **7**, 873 (1995)  
S M Yusuf and L Madhav Rao, *J. Phys.: Condens. Matter* **7**, 5891 (1995)  
M V Subbarao, S M Yusuf, R G Kulkarni and L Madhav Rao, *Pramana – J. Phys.* **53**, 341 (1999)  
A K Rajarajan, S M Yusuf, P Balaya and R G Kulkarni, *Pramana – J. Phys.* **58**, 787 (2002)  
M D Mukadam, S M Yusuf, P Sharma and S K Kulshreshtha, *J. Magn. Magn. Mater.* **269**, 317 (2004)  
N K Prasad, D Panda, S Singh, M D Mukadam, S M Yusuf and D Bahadur, *J. Appl. Phys.* **97**, 10Q903 (2005)  
M D Mukadam, S M Yusuf, P Sharma, S K Kulshreshtha and G K Dey, *Phys. Rev.* **B72**, 174408 (2005)  
[9] S K Paranjpe and S M Yusuf, *Neutron News* **13**, 39 (2002)  
[10] S M Yusuf and L Madhav Rao, *Pramana – J. Phys.* **47**, 171 (1996)  
S M Yusuf and L Madhav Rao, *Neutron News* **8**, 12 (1997)